Membrane Interaction of Chrysophsin-1, a Histidine-Rich Antimicrobial Peptide from Red Sea Bream †

ARTICLE *in* BIOCHEMISTRY · JANUARY 2008

Impact Factor: 3.02 · DOI: 10.1021/bi701344m · Source: PubMed

8 AUTHORS, INCLUDING:

Andrew James Mason
King's College London
49 PUBLICATIONS **1,057** CITATIONS
SEE PROFILE

Philippe Bertani
University of Strasbourg
41 PUBLICATIONS **676** CITATIONS
SEE PROFILE

Alex F Drake
King's College London
72 PUBLICATIONS **1,173** CITATIONS
SEE PROFILE

Antoine Kichler
University of Strasbourg
92 PUBLICATIONS **2,911** CITATIONS
SEE PROFILE

Membrane Interaction of Chrysophsin-1, a Histidine-Rich Antimicrobial Peptide from Red Sea Bream[†]

A. James Mason,*[,‡] Philippe Bertani,[‡] Gilles Moulay,[§] Arnaud Marquette,[‡] Barbara Perrone,[‡] Alex F. Drake,[||] Antoine Kichler,[§] and Burkhard Bechinger[‡]

UMR 7177, Institut de Chimie, Université Louis Pasteur/CNRS, 4 rue Blaise Pascal, 67070 Strasbourg, France, CNRS FRE 3018−Généthon, 1 rue de l'Internationale, BP 60, F-91002, Evry, France, and Department of Pharmacy, King's College London, 150 Stamford Street, London SE1 9NH, United Kingdom

Received July 9, 2007; Revised Manuscript Received October 26, 2007

ABSTRACT: Chrysophsin-1 is an amphipathic α-helical antimicrobial peptide produced in the gill cells of red sea bream. The peptide has broad range activity against both Gram-positive and Gram-negative bacteria but is more hemolytic than other antimicrobial peptides such as magainin. Here we explore the membrane interaction of chrysophsin-1 and determine its toxicity, in vitro, for human lung fibroblasts to obtain a mechanism for its antimicrobial activity and to understand the role of the unusual C-terminal RRRH sequence. At intermediate peptide concentrations, solid-state NMR methods reveal that chrysophsin-1 is aligned parallel to the membrane surface and the lipid acyl chains in mixed model membranes are destabilized, thereby being in agreement with models where permeabilization is an effect of transient membrane disruption. The C-terminal RRRH sequence was shown to have a large effect on the insertion of the peptide into membranes with differing lipid compositions and was found to be crucial for pore formation and toxicity of the peptide to fibroblasts. The combination of biophysical data and cell-based assays suggests likely mechanisms involved in both the antibiotic and toxic activity of chrysophsins.

Our understanding of some of the subtleties in the mechanism of action of cationic antimicrobial peptides is growing (*1*), as is the belief that such peptides may be realistic contenders to be used in the clinical treatment of bacterial or fungal infections that are becoming increasingly resistant to conventional antibiotics (*2*−*4*). For these reasons, it is necessary for the role of each structural motif extant in natural antibiotic peptides to be characterized if we are ever to be in a position to have full control over the properties of future designed antibiotics.

Fish have proven to be a rich source of antimicrobial peptides, where the peptides are apparently secreted to protect against bacterial infection in vulnerable sites such as the gills (*5*−*7*), gastrointestinal tract, and skin (*8*). Three chrysophsin peptides (chrysophsin-1, -2, and -3) have been identified in the gills of the red sea bream, *Chrysophrys major*, which are all bactericidal to pathogenic bacteria at low micromolar concentrations (*9*). Like other antimicrobial peptides found in fish, such as pleurocidin and piscidins (Table 1), the chrysophsins are cationic α-helical peptides that are rich in histidine residues. Unlike these other peptides, however, all three chrysophsins end in an unusual RRRH motif such that, in addition to displaying secondary amphipathicity, where hydrophobic and charged residues are separated by the adoption of secondary helical structure, there is also a considerable change in hydrophobicity between the N and C termini, which could also be considered as a primary amphipathicity (Table 1), where hydrophobic and charged residues are segregated into separate sections of the primary sequence. Chrysophsin has considerable hemolytic activity with an EC_{50}, when challenging human erythrocytes, of approximately 1 μM. This is much greater than that of magainin 2, one of the first cationic helical antimicrobial peptides to be described (*10*), but a little less than that of melittin, a known hemolytic peptide from bee venom (*9*). Antimicrobial peptides, however, have been shown to be effective against *Pseudomonas aeruginosa* by topical applications in rat models. Delivery was occasioned to the lungs by nebulization of the peptide and its subsequent inhalation by the animals (*11*). It follows that the hemolytic activity may not totally prevent the application of a peptide in clinical use. Therefore we were interested to test the toxicity of chrysophsin toward human lung fibroblasts and to determine what role, if any, the C-terminal RRRH sequence played in this toxicity.

By a microculture tetrazolium assay, chrysophsin-1 was found to be extremely toxic to cultured human lung fibroblasts. Interestingly, deletion of the C-terminal RRRH sequence reduced the cellular toxicity approximately 4-fold. To investigate the mechanism of action of the peptide and the contribution of the C-terminal sequence, we performed a detailed biophysical investigation employing fluorescence,

[†] This work was supported by Vaincre la Mucoviscidose (TG-0501). B.P is supported by the FP6 Marie Curie Research Training Network BIOCONTROL (MRTN-CT-2006 033439).

* Corresponding author. Present address: Department of Pharmacy, King's College London, 150 Stamford St., London SE1 9NH, United Kingdom. Tel +44 207 848 4813; fax +44 207 848 4785; e-mail james.mason@kcl.ac.uk.

[‡] Université Louis Pasteur/CNRS.

[§] CNRS FRE 3018−Généthon.

[||] King's College London.

10.1021/bi701344m CCC: $37.00
Published on Web 12/01/2007

Table 1: Sequences of Selected Antibiotic Helical Peptides[a]

peptide	sequence	peptide length	nominal charge at pH 7	nominal charge at pH 5
chrysophsin-1	FFGWL**I**K**G**AI**H**A**G**K**A**I**H**GL**I**H**RRRH**	25	+6	+10
chrysophsin-ΔC	FFGWL**I**K**G**AI**H**A**G**K**A**I**H**GL**I**H	21	+3	+6
chrysophsin-2	FFGWL**I**R**G**AI**H**A**G**K**A**I**H**GL**I**H**RRRH**	25	+6	+10
chrysophsin-3	FIGLLISAG**K**AI**H***D*LI**RRRH**	20	+4	+6
piscidin[b]	FF**HH**IF**R**GIV**H**VG**K**TI**HK**LVTGT	23	+4	+8
pleurocidin	GWGSFF**KK**AA**H**VG**KH**VG**K**AALT**H**YL	25	+5	+8
magainin 2	GIG**K**FL**H**SA**KK**FG**K**AFVG*E*IMNS	23	+4	+5
LAH4-L1	**KK**ALLA**H**AL**H**LLALLAL**H**LA**H**AL**KK**A	26	+5	+9
melittin	GIGAVL**K**VLTTGLPALISWI**KRKR**QQ	26	+6	+6

[a] Residues that are positively charged at pH 7 or 5 are highlighted in boldface type. Negatively charged residues are shown in italic type, while the residues in the synthesized peptides that carry stable isotope labels are underlined. In each case ^{15}N leucine is incorporated at positions 5 and 19, while alanine-d_3 is incorporated at position 12. All the peptides are C-terminally amidated. [b] Piscidin is also known as moronecidin.

circular dichroism (CD),[1] and in particular, solid-state NMR methods similar to those used recently by us to describe the membrane interaction of pleurocidin (*12*). Pleurocidin is a cationic amphipathic antibiotic peptide that causes pore formation in membranes mimicking the bacterial envelope (*13*), but it also seems capable of entering into the bacteria as part of an intracellular targeting bactericidal strategy (*14*). The membrane activity of pleurocidin is enhanced when anionic lipids are included in the membranes, and we demonstrated that pleurocidin interacts preferentially with the anionic lipid component when destabilizing the lipid acyl chains (*12*) during its pore formation (*15*) and likely transmembrane relocation (*16*). Using solid-state NMR techniques on uniformly aligned samples, we demonstrate a surface alignment of chrysophsin similar to that observed for pleurocidin and other similar antimicrobial peptides. In contrast, by using intrinsic tryptophan fluorescence to measure binding of peptide to model membranes, we show that chrysophsin does discriminate between zwitterionic and anionic membranes. However, when chrysophsin is bound to mixed membranes, the disruption of anionic lipid acyl chains is not much greater than that observed for zwitterionic lipids. This indicates that the lipid destabilization is more generalized than that observed for pleurocidin and thereby correlates with the increased toxicity of chrysophsin for eukaryotic cells.

Furthermore, the destabilization of lipid acyl chains by chrysophsin and its C-terminal-deleted derivative, chrysophsin-ΔC, is similar in model membranes mimicking the bacterial environment. However, notable differences in zwitterionic lipid destabilization were observed between the two peptides in both neutral and anionic membranes rich in cholesterol. Large differences in pore formation activity were also observed between the two peptides, with the intact peptide causing much greater release of dye from calcein-loaded vesicles while the truncated peptide was observed to have much reduced helicity in model membranes. Our results are discussed in terms of a model for the antibiotic and, of special interest here, the toxic activity of chrysophsin as well as the implications for selection of structural motifs for novel lead compounds.

[1] Abbreviations: CD, circular dichroism; Fmoc, 9-fluorenylmethyl carbamate; HPLC, high-pressure liquid chromatography; MALDI, matrix-assisted laser desorption/ionization; POPC, 1-palmitoyl-2-oleoyl-3-*sn*-phosphatidylcholine; POPG, 1-palmitoyl-2-oleoyl-3-*sn*-phosphatidylglycerol; POPE, 1-palmitoyl-2-oleoyl-3-*sn*-phosphatidylethanolamine; POPS, 1-palmitoyl-2-oleoyl-3-*sn*-phosphatidylserine; PBS, phosphate-buffered saline; LUV, large unilamellar vesicles; LMV, large multilamellar vesicles; DMEM, Dulbecco's modified Eagle medium; MTT, 3-(4,5-dimethythiazol-2-yl)-2,5-diphenyltetrazolium bromide; FCS, fetal calf serum; TFE, trifluoroethanol; DMSO, dimethyl sulfoxide.

MATERIALS AND METHODS

Peptide and Lipids. Chrysophsin amide (calculated monoisotope molecular weight with stable isotopes = 2895.65) and chrysophsin-ΔC (2290.29) were synthesized by standard Fmoc solid-state chemistry on a Millipore 9050 synthesizer. In crude peptide preparations, a predominant peak was observed upon analysis by HPLC with acetonitrile/water gradients. During HPLC purification, the main peak was collected and the identity of the product was confirmed by matrix-assisted laser desorption ionization (MALDI) mass spectrometry. The lipids 1-palmitoyl-2-oleoyl-3-*sn*-phosphatidylcholine (POPC), 1-palmitoyl-2-oleoyl-3-*sn*-phosphatidylglycerol (POPG), 1-palmitoyl-2-oleoyl-3-*sn*-phosphatidylethanolamine (POPE), 1-palmitoyl-2-oleoyl-3-*sn*-phosphatidylserine (POPS) 1-palmitoyl-d_{31}-2-oleoyl-3-*sn*-phosphatidylcholine (POPC-d_{31}), 1-palmitoyl-d_{31}-2-oleoyl-3-*sn*-phosphatidylglycerol (POPG-d_{31}), 1-palmitoyl-d_{31}-2-oleoyl-3-*sn*-phosphatidylethanolamine (POPE-d_{31}), and cholesterol were obtained from Avanti Polar Lipids, Inc. (Alabaster, AL) and used without further purification. All other reagents were analytical grade or better.

Sample Preparation for Solid-State NMR. For deuterium solid-state NMR, samples with different lipid compositions were prepared (molar ratios in parentheses): POPC/POPC-d_{31}/cholesterol (75:25:30), POPC/POPC-d_{31}/POPS/cholesterol (50:25:25:30), POPE/POPE-d_{31}/POPG (50:25:25), and POPE/POPG-d_{31} (75:25). For the binary and tertiary lipid mixtures, a total of around 5 mg of lipids per sample was dissolved and mixed in chloroform and dried under rotary evaporation at room temperature. In order to remove all organic solvent, the lipid films were exposed to vacuum overnight. The films were then rehydrated with 4 mL of phosphate-buffered saline (PBS) at room temperature. Samples containing peptide were similarly rehydrated with peptide dissolved in PBS. Peptide was added at a final concentration of 2.5 mol % relative to the phospholipid content of the liposomes (i.e., 1 peptide for every 40 phospholipids). Samples were subjected to five rapid freeze−thaw cycles for further sample homogenization and then centrifuged at 21000*g* for 20 min at room temperature. The pellets containing lipid vesicles were transferred to Bruker 4-mm MAS rotors for NMR measurements.

Static aligned samples were prepared by a procedure whereby a sublimable solid is codissolved with the lipids

and peptide to aid alignment during dehydration and rehydration (*17*). Chrysophsin or chrysophsin-ΔC (4 mg), carrying ^{15}N labels at positions Leu5 and Leu19, was codissolved with a solution of POPE/POPG (75:25) or POPC/cholesterol (100:30) in chloroform, at a molar ratio of 2.5 mol % relative to the phospholipid component, that had itself been mixed with a further solution of chloroform containing naphthalene. The molar ratio of naphthalene to lipid was approximately 1:1. The solution was layered over 20 thin glass plates (9 × 22 mm, Marienfeld GmbH, Lauda-Königshofen, Germany) and the plates were then exposed to high vacuum overnight. The samples were rehydrated at 93% humidity and at room temperature.

Tryptophan Fluorescence Spectroscopy. Emission spectra of the intrinsic fluorescence of Trp4 were acquired on a Fluorolog 3-22 spectrometer (Jobin Yvon Horiba, Longjumeau, France) at 310 K. Vesicle suspensions were prepared as for solid-state NMR experiments above in the absence of peptide, except the freeze−thaw cycles were omitted. Vesicles containing POPC/cholesterol (100:30), POPC/POPS/cholesterol (75:25:30), and POPE/POPG (75:25) were prepared at a concentration of 1 mg/mL. An aliquot (150 μL) of these suspensions was added to 0.85 mL of PBS buffer, and then peptide in solution (2 mg/mL in PBS) was added to produce a final peptide concentration of about 0.01 mg/mL. A peptide to lipid molar ratio of 1:40 was maintained. Tryptophan emission spectra of the lipid/peptide suspension were acquired by scanning from 310 to 450 nm, with an excitation wavelength of 295 nm and a spectral bandwidth of 5 nm for both excitation and emission. For fluorescence quenching experiments, 30% acrylamide solution was added stepwise to a final concentration of 0.18 M; at each step equilibration of the sample was ensured, and all spectra are an average of three scans. The temperature was maintained at 310 K by connecting the cuvette holder to an external water bath.

Dye Release Assay. Large unilamellar vesicles (LUV) loaded with calcein were prepared by mechanical extrusion. Three lipid mixtures—POPE/POPG (75:25), POPC supplemented with 30% cholesterol, and POPC/POPS (75:25) supplemented with 30% cholesterol—were dissolved separately in chloroform/methanol. The solutions were dried and then hydrated in PBS buffer (50 mM, pH = 7.4) with 50 mM calcein ions (calcein disodium salt; Fluka) before undergoing several freeze−thaw cycles and then extrusion (11 times) through a 200 nm pore membrane (Avestin). The calcein-entrapped vesicles were separated from the dye solution by gel filtration on a Sephadex G-50 column (2.5 × 3.5 mm) (Sigma) loaded with PBS buffer (50 mM pH = 7.4) supplemented with 75 mM NaCl in order to compensate for the change in osmolarity induced by the presence of calcein molecules and Na^+ counterions. The concentrations of the LUV suspensions eluting from the column were determined by comparing 100% dye release from suspensions before and after the gel-filtration step. Calcein efflux measurements were performed on a Fluorolog 3-22 spectrometer (Horiba Jobin-Yvon, Longjumeau, France). In a typical experiment, an aliquot of the LUV solution was added to 1.5 mL of PBS buffer (50 mM, with 75 mM NaCl, pH = 7.4) in a quartz cuvette and equilibrated for some minutes at 310 K inside the spectrometer. Peptide solution (0.18 mg/mL; (5 μL for chrysophsin, 4 μL for chrysophsin-ΔC) was added into the cuvette while the sample was excited at λ_{exc} = 480 nm and the intensity of fluorescence (I) was recorded at λ_{fluo} = 515 nm for about 10 min. A spectral bandwidth of 1 nm was used for both excitation and emission. The percentage of calcein released from the vesicles ($I_{\%}$) was calculated according to the formula $I_{\%} = 100(I - I_0)/(I_{max} - I_0)$, where I_0 represents the intensity of fluorescence before adding the peptide to the solution and I_{max} is the maximum intensity observed after dissolving the vesicle with 10 μL of 10% Triton X-100. Care was taken to maintain constant I_{max} in order to allow quantitative comparison between the multiple recordings.

Circular Dichroism. For peptide in the presence of vesicles, spectra were acquired on a Jasco J-810 spectrometer with samples maintained at 310 K. For peptide in 50% TFE, spectra were recorded on a Chirascan spectrometer (Applied Photophysics, Leatherhead, U.K.) at room temperature. On the Jasco J-810, spectra were recorded from 250 to 190 nm with a spectral bandwidth of 1 nm and a scan rate of 100 nm/min. On the Chirascan, spectra were recorded from 260 to 180 nm with a spectral bandwidth of 1 nm and a scan rate of 20 nm/min. Samples were prepared as for the tryptophan fluorescence experiments above; however, the POPC/POPG (75:25) lipid suspension was undiluted. Lipid suspension (1 mg/mL; 240 μL) was added to a 1 mm cuvette and then either 12 μL of chrysophsin or 9.44 μL of chrysophsin-ΔC solution (2 mg/mL) was added with thorough mixing. CD spectra were not obtained for either POPE/POPG or POPC/cholesterol vesicles, as these lipids induced light scattering or had contributions from the lipid that caused the obtained spectra to be unreliable. Sonication of the lipid suspensions to form small unilamellar vesicles (SUV) did not improve the quality of the spectra for any of the model membrane systems. To obtain spectra in the presence of 50% trifluoroethanol (TFE), 100 μL of peptide solution (0.25 mg/mL) was mixed with 100 μL of TFE. A spectrum of either the peptide-free lipid suspension or TFE was subtracted, and for the experiments performed in the presence of lipid vesicles, Means Movement smoothing with a convolution width of 5 points was applied. Secondary structure analysis of the spectra between 185 and 240 nm (50% TFE) or 197 and 240 nm (PC/PG) was performed by use of CDPro (*18*) and the reference data sets SMP50 and SMP56, respectively. The difference between the average helical values provided by the three methods in CDPro (CONTINLL, SELCON3, and CDSSTR) was assessed by ANOVA (*19*) to determine whether the reduction in helical content is significant.

Solid-State NMR. ^{2}H quadrupolar echo experiments (*20*) for samples containing either POPC-d_{31}, POPE-d_{31}, or POPG-d_{31} as labeled lipid were performed at 46.10 MHz on a Bruker Avance 300 NMR spectrometer with a 4 mm MAS probe, spectral width of 200 kHz, and recycle delay, echo delay, acquisition time, and 90° pulse lengths of 0.3 s, 42 μs, 2 ms, and 5 μs, respectively. The temperature was maintained at 310 K to keep the bilayers in their liquid-crystalline phase. During processing, the first 40 points were removed in order to start Fourier transformation at the beginning of the echo. Spectra were zero-filled to 8K points and 50 Hz exponential line-broadening was applied. Smoothed and/or averaged deuterium order parameter profiles were obtained from symmetrized and dePaked ^{2}H NMR powder spectra by published procedures (*21*−*23*). Spectra were also obtained

for both peptides in unlabeled lipids to account for signal from ^{2}H-labeled Ala12; however, no signal that could be attributed to this label was observed.

^{15}N cross polarization (CP) spectra of static aligned samples were acquired at 40.54 MHz for ^{15}N on a Bruker Avance 400 NMR spectrometer equipped with a double-resonance flat-coil probe. An adiabatic CP pulse sequence was used with a spectral width, acquisition time, CP contact time, and recycle delay time of 25 kHz, 10 ms, 800 μs, and 3 s, respectively. The ^{1}H $\pi/2$ pulse and spinal64 heteronuclear decoupling field strengths were 42 kHz. A total of 40K scans were accumulated; the spectra were zero-filled to 4K points and 100 Hz exponential line-broadening was applied during processing. Spectra were externally referenced to $^{15}NH_4Cl$ at 41.5 ppm.

^{31}P spectra with proton decoupling were acquired at 161.953 MHz for ^{31}P on a Bruker Avance 400 NMR spectrometer equipped with a double-resonance flat-coil probe. Proton-decoupled ^{31}P spectra were acquired with one 4-μs 90° pulse, followed by continuous-wave heteronuclear ^{1}H decoupling at a field strength of 40 kHz. The spectral sweep width was 75 kHz, and the recycle delay and acquisition times were 5 s and 6.8 ms, respectively. The temperature was maintained at 303 K. Spectra were zero-filled to 16K points and 50 Hz exponential line broadening was applied during processing. Spectra were referenced externally to 85% H_3PO_4 at 0 ppm.

MTT Assay. Cytotoxicity was evaluated by performing the 3-(4,5-dimethythiazol-2-yl)-2,5-diphenyltetrazolium bromide (MTT; Sigma) assay (*24*). Dulbecco's modified Eagle medium (DMEM; Gibco−BRL) was supplemented with 2 mM L-glutamine, 100 units/mL penicillin, 100 μg/mL streptomycin, and 10% fetal calf serum (FCS; HyClone). A total of 90 000 human fetal lung fibroblasts (MRC-5) or 120 000 SV40-transformed human fetal lung fibroblasts (MRC-5 V2) per well were plated in 24-well plates (Costar) 1 day before the assay. The cells were incubated with peptide solutions for 4 h in the presence or absence of 10% FCS. Cells were incubated with 1% Triton X-100 as a positive control (100% toxicity), while untreated cells were used as a negative control. The cell culture medium was then removed and replaced by serum-free DMEM (450 μL) and 50 μL of MTT (5 mg/mL in PBS), and the cells were incubated at 37 °C for 2 h. The medium was then removed; 500 μL of dimethyl sulfoxide (DMSO) was added to each well, to dissolve the formazan crystals produced from the reduction of MTT by viable cells, and the absorbance was measured at 570 nm.

RESULTS

Peptide Design. Of the three chrysophsin peptides (*9*) (Table 1), we selected chrysophsin-1 for this study. Chrysophsin-2 is identical to chrysophsin-1 with the exception that lysine at position 7 is replaced by an arginine. Chrysophsin-3 is somewhat shorter at 20 residues and contains a serine and an aspartate residue that are not found in the other two peptides. All three peptides possess the same RRRH sequence at the C-terminus, with the C-terminal histidine being amidated in nature. Two peptides were synthesized for this study (Table 1): chrysophsin-1, to be known simply as chrysophsin hereafter, and a truncated peptide chrysophsin-ΔC, where the C-terminal RRRH sequence was deleted. Both peptides were amidated at the C-terminus. It is possible that a certain peptide length is necessary for antibiotic activity, but it is notable that it has been shown that cationic α-helical peptides maintain antibiotic activity with sequences as short as 14 residues (*25*).

Table 2: Toxicity Study of Three Antibiotic Peptides As Determined by MTT Assay[a]

	EC_{50} (μM)			
peptide	MRC5	MRC5 (FCS)	MRC5-V2	MRC5-V2 (FCS)
chrysophsin	4.6	8.5	4.8	9.6
chrysophsin-ΔC	20.5	34.8	17.3	28.1
LAH4-L1	>92[b]	>92[b]	24.7	>92[b]

[a] Human lung fibroblasts (MRC5) and SV40 virus transformed fibroblasts (MRC5-V2) were challenged in the presence or absence of fetal calf serum (FCS). [b] Maximum peptide concentration tested was 256 μg/mL.

Toxicity toward Human Lung Fibroblasts. Human lung fibroblasts were challenged with both the full-length and truncated peptide and also a model histidine-rich peptide, LAH4-L1, which has modest antibiotic activity at neutral pH (*26*). Both chrysophsin peptides are decidedly toxic to human fibroblasts in culture at low micromolar concentrations (Table 2). This finding is in stark contrast with that observed for the model peptide, which was toxic only to fibroblasts that had been transformed with SV40 virus (MRC5-V2) and then only upon incubation in the absence of serum. The presence of serum in the culture medium does reduce the toxicity of the chrysophsin peptides but only modestly, by a factor of between 1.6 and 2. Equally, almost no selectivity was observed between the MRC5 and MRC5-V2 cells. Interestingly, however, there was a notable difference between the toxicity of chrysophsin and the truncated chrysophsin-ΔC, as removal of the RRRH sequence reduced the toxicity by between 2.9 and 4.4 times depending on the cell line and conditions.

Circular Dichroism. The initial characterization of chrysophsin revealed that the peptide adopted an α-helical structure in the presence of the helix-promoting solvent TFE (*9*). Analysis of the helical wheel diagram for chrysophsin (Figure 1), however, indicates that although a perfect amphipathic helix can be formed at the N-terminal segment, this secondary amphipathicity would break down toward the C-terminus if the peptide were to adopt a perfect α-helical secondary structure throughout its full length. The effect, therefore, of deleting the C-terminal RRRH sequence might be to increase the average helicity of the peptide. Circular dichroic (CD) measurements of the two peptides, either in 50% TFE or in the presence of lipid vesicles, provide information on the average secondary structure adopted by the peptides. Chrysophsin is known to adopt an α-helical structure in the presence of TFE, while in aqueous solution the peptide is unstructured (*9*), and this is confirmed by our measurements since the spectra obtained for chrysophsin and chrysophsin-ΔC are both characteristic spectra of proteins with considerable α-helix content (Figure 2A). Analysis of the spectra with the CDPro software (*18*) provides a numerical estimate of the helical content (Table 3). However, the choice of both reference sets and analysis method introduces some variation in the reported values, and hence in the present study only an essentially qualitative view of the helical content is

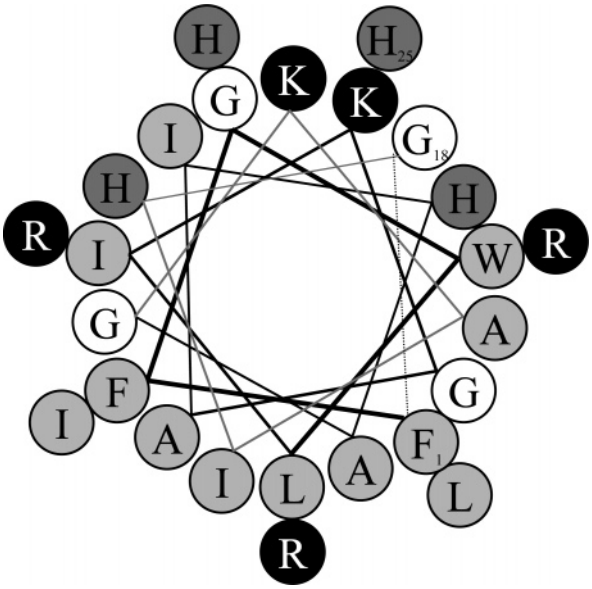

FIGURE 1: Helical wheel diagram highlighting the effect of the RRRH C-terminal sequence on the amphipathic nature of the peptide. At the N-terminal end of the peptide the amphipathic separation of hydrophobic and charged residues is preserved, but at the C terminal end such separation would be impossible if the peptide remained a perfect α-helix.

obtained. In 50% TFE, the α-helical content of chrysophsin is very high with only a small proportion of the peptide experiencing a nonhelical structure, mostly random coil. However, when the peptide is truncated, the molar ellipticity in the region between 205 and 235 nm is strongly affected (Figure 2A) and the helical content, as determined by each of the three methods within the CDPro package, drops significantly, with a concomitant rise in predominantly random coil and also turn conformations. On average, therefore, chrysophsin-ΔC has less α-helical content than its full-length parent peptide even in the presence of the helix-stabilizing solvent TFE. In the presence of POPC/POPG (75:25) large multilamellar vesicles (LMV), both peptides retain a largely α-helical conformation (Figure 2B), but the percentage helical content is reduced compared with 50% TFE. Although the quality of the spectra and the subsequent analysis is impaired by light scattering, with the result that only the region between 197 and 250 nm can be analyzed, the difference between the spectra obtained for the truncated and full-length peptides in the lipid environment is sufficient to support the view that the reduction in helical content observed for the truncated peptide in 50% TFE is maintained in the membrane-mimicking lipid environment.

Tryptophan Fluorescence Spectroscopy. Intrinsic fluorescence of the tryptophan residue located at position 4 in chrysophsin or chrysophsin-ΔC can be used as a sensitive reporter of the environment experienced by the peptide when interacting with vesicles of varying lipid compositions. Three parameters from the fluorescence experiments are used here to characterize the peptide−lipid interactions. Emission maxima, emission intensity, and accessibility to the aqueous quencher acrylamide all provide information on the location of the tryptophan residue of the peptide, where values with shorter wavelengths, greater intensity, and reduced accessibility represent a more hydrophobic environment, as is found within the hydrophobic core of the membrane. Emission spectra of chrysophsin in aqueous solution are characterized by a maximum at 360 nm (Figure 3A), but when the peptide is incubated with lipid vesicles the maximum is shifted to shorter wavelengths and is of increased intensity, indicating that in all cases chrysophsin interacts with the model membranes and is located in a more hydrophobic environment than when it is free in solution. Clear differences in both emission maxima and intensity, however, can be observed for spectra acquired of chrysophsin in the presence of the three differing lipid mixes. The smallest blue shift and least intense maximum is observed for chrysophsin in the presence of vesicles composed of POPC/cholesterol. When the anionic lipid POPS is added to this membrane, the intensity of the maximum increases dramatically with a concomitant shift in the maximum from 350 to 343 nm. This apparent selectivity of chrysophsin for membranes containing anionic lipids is supported by the Stern−Volmer plot (Figure 3C), where the accessibility of the tryptophan to aqueous quencher is plotted. In the presence of neutral POPC/cholesterol membranes, chrysophsin is far more accessible to acrylamide than when either of the anionic lipid membranes is present. The POPE/POPG lipid mix is included as a model for bacterial membranes; this approximately reflects the lipids present in *Escherichia coli* (*27*). The fluorescence emission spectra of chrysophsin in the presence of such membranes indicate that the peptide resides in a relatively hydrophobic environment since the emission maximum is again shifted to the shorter wavelength of 340 nm and the intensity of the maximum is enhanced, although not to the same degree as when POPC/POPS/cholesterol liposomes are present. The hydrophobic nature of the peptide location is confirmed, however, by the Stern−Volmer plot of accessibility to aqueous quencher (Figure 3C). Similar spectra were obtained for chrysophsin-ΔC under the same conditions (Figure 3B) with the exception of the spectrum obtained in the presence of the zwitterionic POPC/cholesterol membranes. In this case, the difference in intensity between spectra acquired in the presence of liposomes either containing or lacking in POPS was reduced when compared with the same spectra obtained for chrysophsin, while the Stern−Volmer plot (Figure 3C) indicated a much reduced accessibility to aqueous quencher for the truncated peptide when compared with the full-length peptide. Taken together, these data suggest that removing the RRRH sequence from the C-terminus removes the selectivity between anionic and zwitterionic membranes from the peptide. Furthermore since the fluorescence intensities and maxima are not exactly correlated (Figure 3B), it is likely that these are also sensitive to ordering due to secondary structure formation around the tryptophan residue. Therefore the fluorescence data also suggest that the tryptophan residue is likely to be located in the helical region; that is, the helix in chrysophsin-ΔC is located toward the N-terminus.

^{2}H Solid-State NMR. Recently, a molecular dynamics study of the behavior of cationic amphipathic antimicrobial peptides in model membranes has linked the localized disruption of lipids, and in particular the lipid acyl chains, to the formation of a water-filled gap across the membrane, which was termed a disordered toroidal pore (*16*). A detailed picture of the effect of the peptides on the lipid chains in model membranes can be obtained experimentally by acquiring wide-line ^{2}H echo spectra (*28*) of the lipid mixes in the absence and presence of chrysophsin or chrysophsin-ΔC.

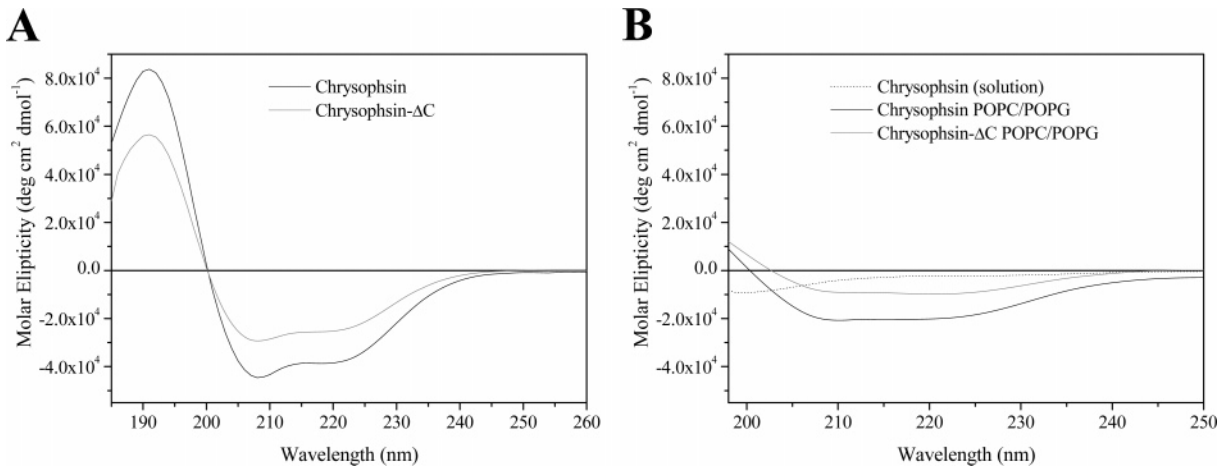

FIGURE 2: CD spectra of chrysophsin and chrysophsin-ΔC in 50% TFE (A) or in the presence of POPC/POPG (75:25) liposomes (B) at a peptide to lipid ratio of 1:40, neutral pH, and 310 K.

Table 3: Comparison of α-Helical Content of Chrysophsin and Chrysophsin-ΔC[a]

		fraction α-helix			
peptide	environment	CONTINLL	SELCON3	CDSSTR	avg
chrysophsin	50% TFE	0.78	0.89	0.83	0.83
chrysophsin-ΔC	50% TFE	0.52	0.61	0.72	0.62
chrysophsin	PC/PG	0.45	0.54	0.60	0.53
chrysophsin-ΔC	PC/PG	0.31	0.31	0.32	0.31

[a] α-Helical content was compared in differing environments as determined by analysis of the CD spectra (Figure 2) between 190 and 240 nm by use of reference set SMP50 (50% TFE) or 197 and 240 nm and set SMP56 (PC/PG) by the CDPro software package. Three methods are used in the package. Differences in average helix content between the full length and truncated peptide are significant at $p < 0.05$.

Furthermore, a variety of deuterated lipids is available, so it is possible to determine the effect of peptide binding, in a differential manner, on both the anionic and zwitterionic components of mixed membranes.

The addition of chrysophsin or chrysophsin-ΔC to membranes composed of POPE/POPG-d_{31} causes a noticeable reduction in the quadrupolar splittings observed for labeled sites throughout the acyl chain of the anionic lipid, where the largest splittings correspond to the labels closest to the polar head-groups with the smallest splittings attributable to the tail (Figure 4A,B). Calculation of the smoothed order parameter profiles for the lipid chain reveals that the order is markedly reduced, and when plotted relative to the order profile obtained for peptide-free liposomes, the reduction in order is proportionally greatest in the lower part of the chain, corresponding to the hydrophobic center of the lipid bilayer (Figure 4E). Performing the same experiments where the zwitterionic POPE carries the deuterium labels shows how the peptides interact with the neutral lipids (Figure 4C,D). The reduction in order for the zwitterionic lipids is a little less than that observed for anionic POPG-d_{31} (Figure 4F). In both cases, however, the differences observed for the effects of the two peptides are modest, with chrysophsin having a slightly greater effect than chrysophsin-ΔC on the anionic component while the situation is reversed when the zwitterionic component is observed (Figure 4E,F). This is in stark contrast to the effect observed in our previous study of pleurocidin, where the anionic lipids were clearly destabilized in preference to the zwitterionic lipids (*12*).

For membranes composed of POPC/cholesterol, with or without anionic POPS, the effect of addition of chrysophsin or chrysophsin-ΔC on the quadrupolar splittings, and hence the calculated order parameter profiles, is rather different (Figure 5E). When chrysophsin is added to neutral POPC/cholesterol membranes (Figure 5A), almost no change in splittings or order can be discerned. In contrast, the addition of chrysophsin-ΔC (Figure 5B) does cause a modest reduction in order throughout the chain of the zwitterionic POPC-d_{31}, which is slightly more pronounced in the lower portion of the chain. When POPS is incorporated into the membranes, both chrysophsin and chrysophsin-ΔC induce a reduction in the size of the quadrupolar splittings (Figure 5C,D), though it is revealed by comparison of the order parameter profiles that again the effect of chrysophsin on the zwitterionic lipid is more modest than that of chrysophsin-ΔC. Taken together, the deuterium solid-state NMR data provide further support for a role for the RRRH sequence in discriminating between neutral and negatively charged membranes but show that the lipid disruption induced by both chrysophsin and chrysophsin-ΔC is more general that that induced by, for example, pleurocidin.

Dye Release. The ability of each of the two chrysophsin peptides to induce pore formation was assessed by quantifying the release of calcein from vesicles of varying lipid composition when challenged by either chrysophsin or chrysophsin-ΔC (Figure 6). In all cases chrysophsin induced greater dye release than chrysophsin-ΔC. Addition of both peptides causes a rapid release of dye from POPE/POPG vesicles (Figure 6A); however, the amount of dye released after addition of chrysophsin is much greater than that released after addition of chrysophsin-ΔC. When liposomes are prepared with POPC/cholesterol, the percentage of dye release is rather low; in the case of chrysophsin-ΔC, dye release is negligible after 10 min of incubation, while the full-length peptide causes less than 20% dye to be released (Figure 6B). Both peptides become more active when anionic POPS is incorporated into the membranes, although the activity of chrysophsin-ΔC remains low and releases only slightly more than 5% dye over the 10 min time course of the experiment. Chrysophsin, however, does display considerable activity toward these anionic but sterol-rich membranes and is capable of liberating more than 25% of the dye over the same period.

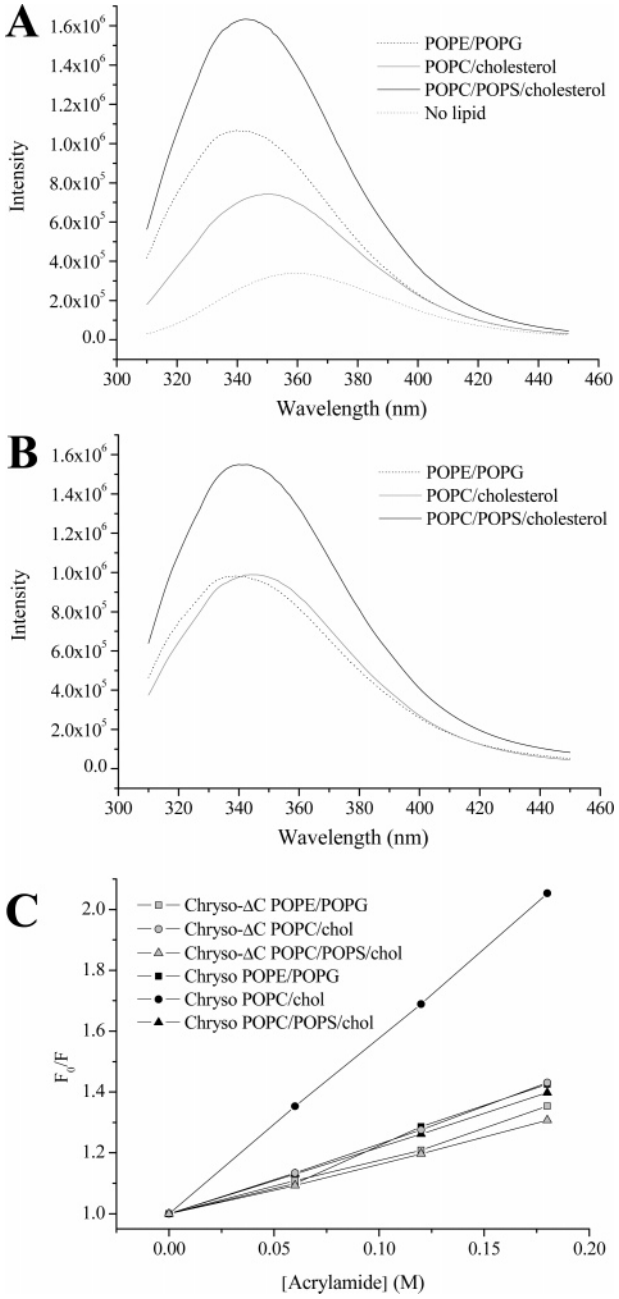

FIGURE 3: Intrinsic tryptophan fluorescence spectra of Trp4 of chrysophsin (A) or chrysophsin-ΔC (B) at neutral pH, 310 K, in solution or in different liposomes comprising POPE/POPG, POPC/cholesterol, or POPC/POPS/cholesterol at a peptide to lipid ratio of 1:40. Stern−Volmer plots (C) of the effect of adding an aqueous acrylamide quencher reveals the depth of chrysophsin penetration into the same liposomes.

^{15}N Solid-State NMR of Aligned Membrane Samples. The preparation of samples containing chrysophsin or chrysophsin-ΔC simultaneously labeled with ^{15}N at positions Leu5 and Leu19 and aligned on glass plates and the subsequent measurement of the static proton-decoupled ^{15}N cross polarization solid-state NMR spectrum allows an accurate determination of the value of the anisotropic chemical shift (Figure 7). The resonances can be fitted with single mixed Gaussian−Lorentzian curves located between 71.4 and 92.9 ppm, indicating that the long axes of each of the peptide helices are oriented parallel to the membrane surface. Each peak is a result of the contributions from two residues, but analysis by a peak-fitting routine did not show any clear indication of shoulders or multiple components, while the quality of the fits was scarcely improved when two peaks were fitted to each resonance, indicating that the two labeled sites in the peptide adopt a similar orientation: The resonance full width at half-height (fwhh) for each peak is large and constitutes a spread of orientations and is a reflection of the severe disruption of the membranes induced by the peptide. The intense resonance observed around 23 ppm in the static ^{31}P spectra (Figure 8) of the same samples confirmed that the membranes remained aligned and intact; however, the appearance of a contribution to the spectra at around −10 ppm indicated considerable disruption of the lipid headgroup alignment, much greater than that observed with pleurocidin (*12*), in agreement with the more general lipid disruption observed above. Notably, the disruption of the phospholipid headgroup alignment caused by chrysophsin was greater in both cases than for chrysophsin-ΔC, while the effect was more noticeable for the membranes composed of POPE/POPG (Figure 8A) than POPC/cholesterol (Figure 8B), in agreement with the ensemble of the data described above. The increased spread of orientations observed for the phospholipids does, however, rule out a more detailed analysis of the peptide tilt beyond indicating the surface alignment of the peptide long axes (*29*, *30*).

DISCUSSION

Mechanism of Antibacterial Action. Recently, we have characterized the membrane interaction of both natural (*12*) and designed (*26*) histidine-rich cationic antimicrobial peptides with model membranes to ascertain their mechanism of action against bacteria. In common with a number of other cationic amphipathic peptides, including magainin and piscidins (*31*, *32*), these studies revealed that the peptides adopt a surface alignment when in their most active conformation and strongly disrupt the lipid acyl chain order of the anionic lipid component of mixed membranes (*12*, *26*). The data are in line with previous suggestions where linear cationic peptides form amphipathic structures localized in the membrane interface when interacting with lipid bilayers and can result in a variety of macroscopic phases similar to mixtures between lipids and other amphiphiles. Depending on the experimental conditions, the behavior of such detergent-like molecules can vary from stabilizing the membranes to lysis and is best described by phase diagrams in which specific models represent specific phases (*33*, *34*). Here the lipid interactions of chrysophsin were studied at peptide lipid ratios where pleurocidin permeabilizes lipid membranes (*35*) and yet the bilayers remained otherwise intact despite the apparent localized disruption of the lipid chains. The experimental solid-state NMR data from these two studies fits well with both a recent fluorescence study of the mechanism of action of an amphipathic cell-penetrating peptide (*36*) and also a recent in silico study of the interaction of magainin H2 with a model lipid bilayer (*16*). At similar peptide to lipid ratios, a disordered toroidal pore forms where the peptide retains an alignment approximately parallel to the membrane surface and is able to migrate from one bilayer leaflet to the other (*16*). The consequences of this for the bacteria are at least 2-fold. First, a pore is formed in the membrane such that cell contents are released and any electrochemical gradient is attenuated. Second, the localized lipid disruption may facilitate the entry of the peptide into

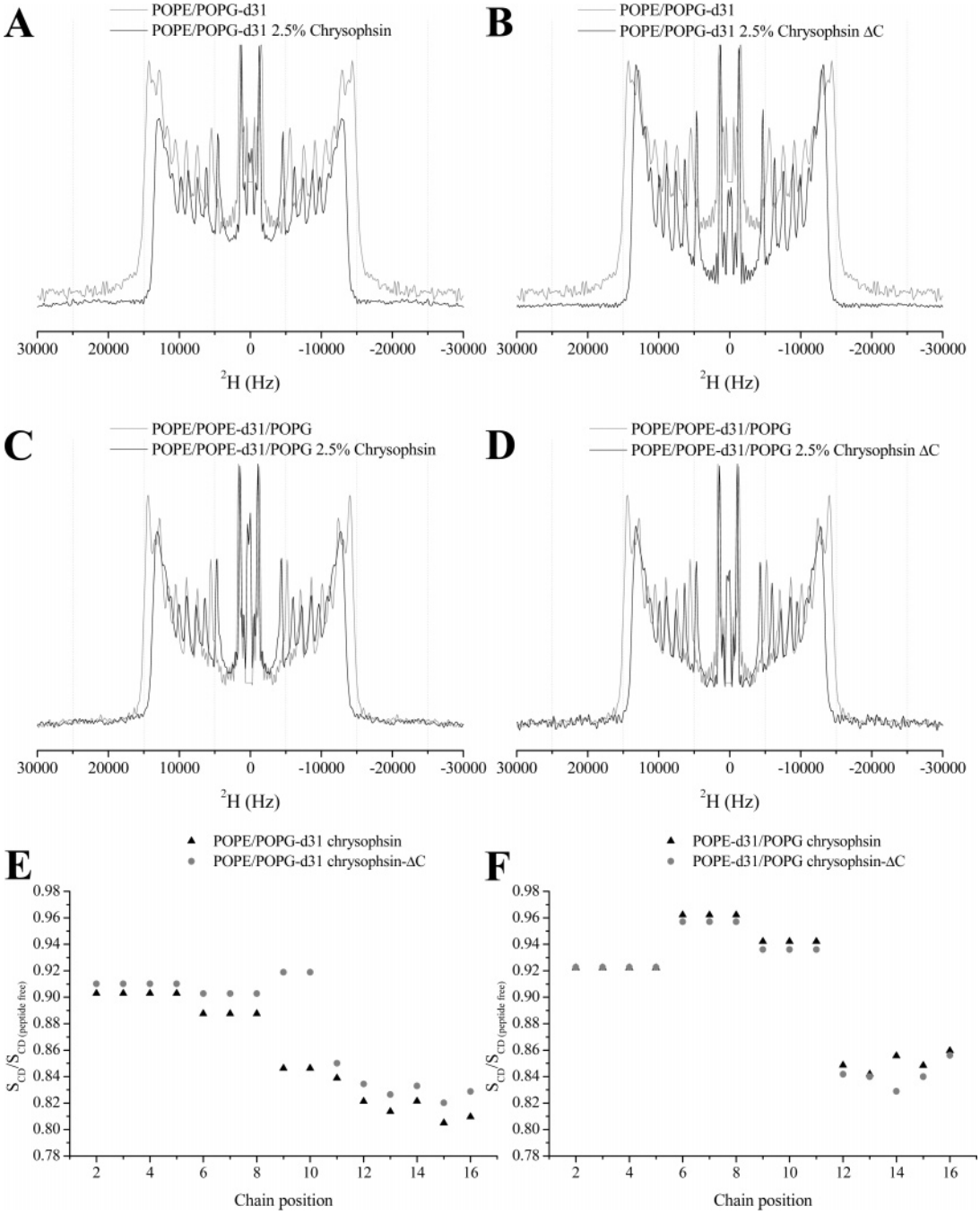

FIGURE 4: Effect of adding chrysophsin (A, C) or chrysophsin-ΔC (B, D) to liposomes containing POPE/POPG-d_{31} (A, B) or POPE/POPE-d_{31}/POPG (C, D) as observed by acquiring ^{2}H spectra of the deuterium-labeled anionic POPG-d_{31} or zwitterionic POPE-d_{31}. Spectra were recorded on a Bruker Avance 300 spectrometer at 310 K. Spectra of liposomes are shown in the absence (gray lines) and presence (black lines) of 2.5 mol % peptide. Smoothed order parameters obtained for spectra incubated with 2.5 mol % peptide are shown calculated relative to profiles for peptide-free liposomes containing POPE/POPG-d_{31} (E) and POPE-d_{31}/POPG (F).

the bacteria where it may seek out an intracellular target, a property that has been observed for a number of antibiotic peptides (*1*) in addition to pleurocidin (*14*).

The data in the present study largely support the current model but with some differences. Both chrysophsin and chrysophsin-ΔC adopt a surface alignment in either anionic or neutral mixed membranes. Both peptides also strongly reduce lipid acyl chain order in mixed POPE/POPG membranes, a feature that accompanied transient pore formation in a previously proposed model (*34*, *35*) and was visualized in detail in the recent in silico study (*16*). Addition of cationic amphipathic peptides in larger quantities will likely cause the formation of micellar or bicellar type phases (*37*−*39*). However, unlike pleurocidin and the designed peptides based on LAH4, both chrysophsin-ΔC and, to a slightly lesser extent, chrysophsin also have a more notable effect on the zwitterionic component of such membranes. In each POPE/POPG sample prepared for ^{2}H-solid-state NMR only 25% of the lipids carry deuterium labels, and in the case of pleurocidin, the differential effect of the peptide on the labeled POPG and POPE indicates that the anionic lipid accumulates in the neighborhood of this peptide. In this study, since the effect of peptide on the lipid chain order for both lipids is similar, it is likely that unlabeled POPE lipids exchange with their labeled analogues such that the disruption of acyl chain order induced by chrysophsin and, in particular,

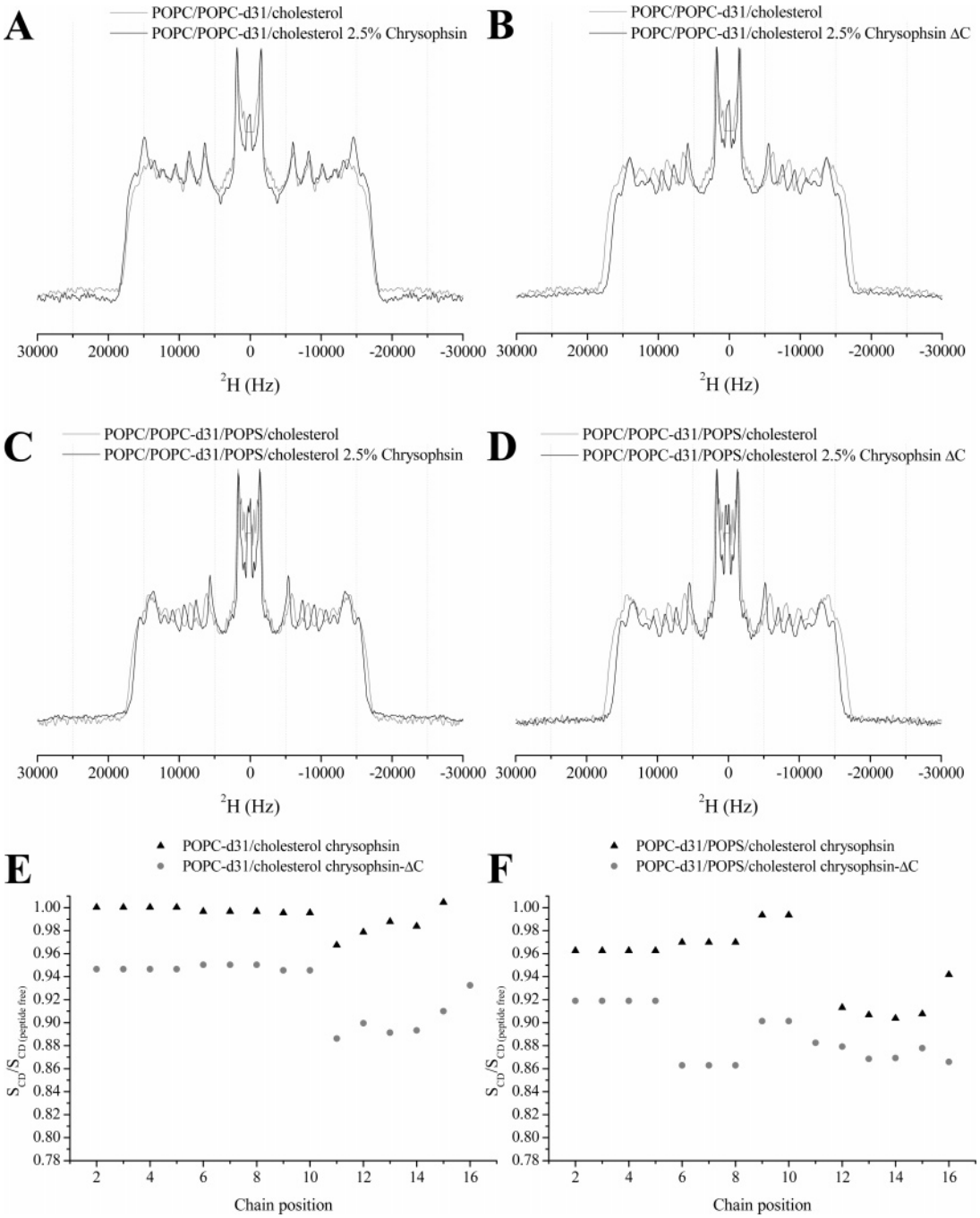

FIGURE 5: Effect of adding chrysophsin (A, C) or chrysophsin-ΔC (B, D) to liposomes containing POPC/POPC-d_{31}/cholesterol (A, B) or POPC/POPC-d_{31}/POPS/cholesterol (C, D) as observed by acquiring ^{2}H spectra of the deuterium-labeled zwitterionic POPC-d_{31}. Spectra were recorded on a Bruker Avance 300 spectrometer at 310 K. Spectra of liposomes are shown in the absence (gray lines) and presence (black lines) of 2.5 mol % peptide. Smoothed order parameters obtained for spectra incubated with 2.5 mol % peptide are shown calculated relative to profiles for peptide-free liposomes containing POPC-d_{31}/cholesterol (E) and POPC-d_{31}/POPS/cholesterol (F).

chrysophsin-ΔC is rather more generalized. This generalized disruption is also reflected in the quality of the ^{15}N spectra obtained for aligned samples where the peptide disturbs the lipids around it and consequently adopts a considerable distribution of orientations leading to a rather broad signal.

Mechanism of Toxicity to Cultured Fibroblasts. The mechanism of action of antimicrobial or anticancer peptides against eukaryotic cells has not been studied in great detail, and a variety of membrane interactions could play a role when cationic amphipathic peptides challenge eukaryote cells. First, the peptides could disrupt the plasma membrane, leading to a general release of cell contents and loss of cell integrity. Second, the peptides could either cross the plasma membrane or be internalized by an endocytotic process and attack intracellular targets. Recently, peptides such as lactoferricin have been investigated as potential anticancer agents and it has been shown that this peptide enters neuroblastoma cells and depolarizes mitochondrial membranes (*40*). This initiates a number of necrotic and apoptotic processes, but ultimately the main events leading to cell death are the destabilization of the cell membrane and the collapse of the outer and inner mitochondrial membranes. Our biophysical data supports such a mechanism in a number of ways. Transformed cells often display elevated levels of anionic

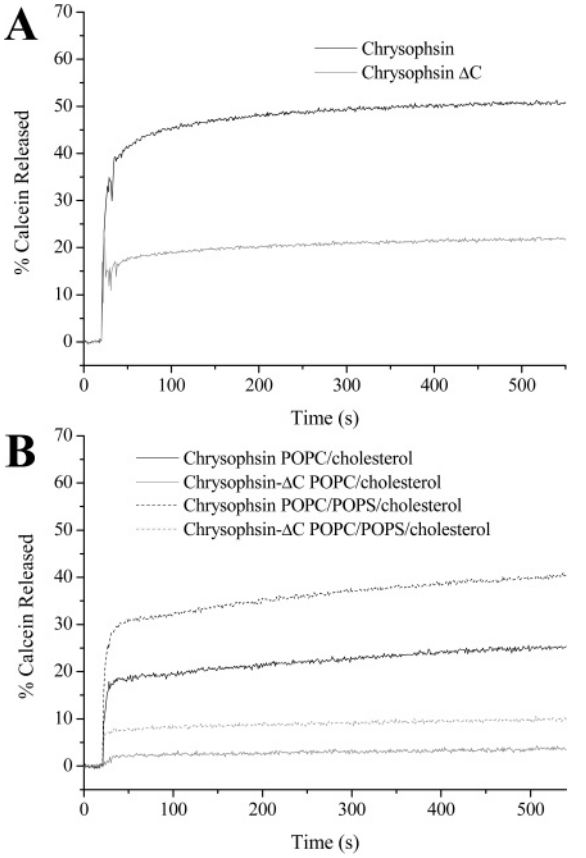

FIGURE 6: Comparison of pore formation in POPE/POPG (A), POPC/cholesterol (solid lines, B) or POPC/POPS/cholesterol (dashed lines, B) liposomes, assessed by monitoring the release of fluorescent calcein from large unilamellar vesicles when challenged with chrysophsin and chrysophsin-ΔC. The experiment was performed at 310 K and pH 7.4. Triton X-100 was added to terminate the experiment and to allow quantification of 100% calcein release.

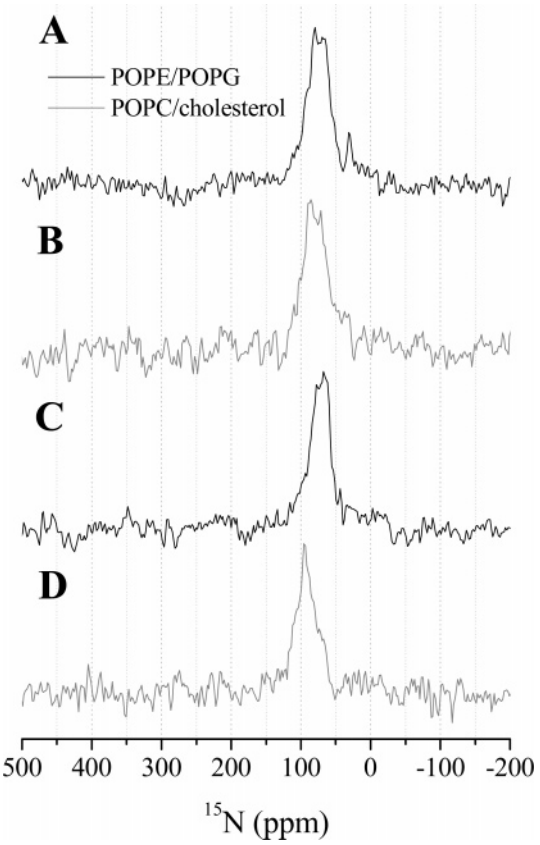

FIGURE 7: Static ^{15}N NMR of 2.5 mol % chrysophsin (A, B) or chrysophsin-ΔC (C, D) in aligned POPE/POPG (A, C) or POPC/cholesterol (B, D) membranes, indicating a surface alignment of the peptides in all cases.

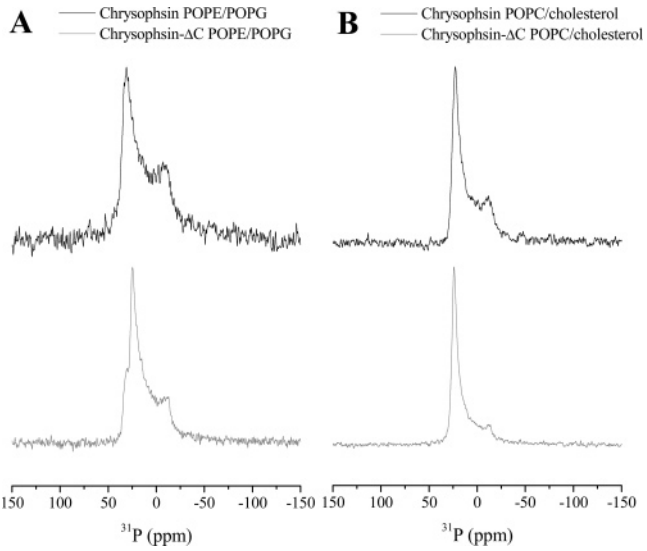

FIGURE 8: Static ^{31}P NMR of 2.5 mol % chrysophsin or chrysophsin-ΔC in aligned POPE/POPG (A) or POPC/cholesterol (B) membranes, showing the response of macroscopic alignment of the phospholipid headgroups to the presence of the two peptides.

phosphatidylserine at their surface (*41*) and this has been exploited in the design of anticancer peptides that demonstrate selectivity for transformed over normal cells. In a parallel study we have shown that selectivity of the order of between 2 and 4 times is possible between MRC5 and MRC5-V2 cells (*42*), yet in the present study, neither chrysophsin nor chrysophsin-ΔC is more toxic to MRC5-V2 cells, which are the same MRC5 lung fibroblasts transformed with SV40 virus (*43*). The ^{2}H NMR data shows that when anionic lipids are present in the membrane, the interaction of both chrysophsin and chrysophsin-ΔC with those membranes is enhanced and the lipids are more strongly destabilized, even in the presence of cholesterol. The dye release study shows that adding anionic POPS to the membranes increases the ability of both peptides to induce pore formation. Crucially, however, chrysophsin-ΔC, though it binds quite effectively to neutral membranes, is incapable of forming pores and is only quite weakly active against the same membranes when enriched with anionic POPS, yet it remains rather toxic to both cell types. Both peptides are more active against the POPE/POPG membranes and cause far greater dye release from these membranes where there is no sterol present. Recently we have shown that sterols effectively modulate the membrane-disrupting behavior of cationic antimicrobial peptides with elevated levels of cholesterol, dramatically reducing the ability of pleurocidin to destabilize lipids and cause pore formation (*15*). Therefore, membranes containing reduced levels of sterol and elevated levels of anionic lipids would be more likely targets for such peptides. Mitochondrial membranes are composed of a mixture of phospholipids and sterols but the cholesterol content of the outer and, in particular, inner mitochondrial membranes is much reduced in comparison with the plasma membrane (*44*). Furthermore, anionic cardiolipin and phosphatidylinositol comprise 18% and 13%,

respectively, of the phospholipids in the inner and outer mitochondrial membranes of mammalian cells (*45*). The different levels of toxicity observed between the full-length peptide and the truncated version might therefore purely be ascribed to their ability to disrupt the lipids and permeabilize such membranes, yet other factors may contribute. First, greater membrane destabilization may often be linked to higher pore formation activity, but as will be discussed below, this is not always the case. An alternate result of the disruption of lipid acyl chains is a greater movement of the peptide from one leaflet of the bilayer to another (*16*). As a greater disruption of POPC-d_{31} lipid acyl chains is observed for chrysophsin-ΔC in neutral membranes compared with chrysophsin, this could signify that a greater amount of truncated peptide can cross either neutral plasma or endosomal membranes than the full-length peptide and hence enter the cell. Conversely, chrysophsin may actually be more effective than chrysophsin-ΔC at entering cells and this may underpin the enhanced toxicity of the full-length peptide. The unusual RRRH sequence could promote uptake of the peptide by endocytosis since it has been shown that polyarginine is far more effective at entering cells than polymers composed of other cationic residues including lysine and histidine (*45*), and the truncated peptide is completely lacking in arginine. Further data concerning the mechanism of toxicity to eukaryote cells by cationic histidine-rich peptides will be presented elsewhere (*42*).

Structure−Function Relationships in Chrysophsin. The comparison of the membranes activities of chrysophsin and chrysophsin-ΔC allows some interesting features of the activity of such cationic amphipathic helices to become apparent. Fluorescence emission spectra of the tryptophan residue in both peptides reveal the likely membrane location of the peptide in membranes of differing composition. Removal of the RRRH C-terminal sequence leads to an increased affinity of the truncated peptide for neutral and cholesterol-rich membranes characterized by a more hydrophobic location of chrysophsin-ΔC compared with chrysophsin in POPC/cholesterol. This is supported by solid-state NMR of deuterium-labeled POPC in neutral POPC/cholesterol membranes where only the truncated peptide causes any disruption of lipid chain order. This demonstrates that the highly charged RRRH segment could be responsible for reducing interactions with neutral membranes in the parent peptide. A simple explanation for this observation is derived from the electrostatic repulsion between peptides. Once the first peptides have partitioned into the membrane, the surface becomes cationic and repels the positively charged molecules remaining in solution from the surface (*46*). Equally, the enhanced affinity of the truncated peptide for such membranes may be related to a reduction of an "image charge" effect (*47*) where the lower charge of the truncated peptide reduces the unfavorable electrostatic interaction between the charged peptide and the hydrophobic interior of the membrane. Removal of this segment also strongly affects the permeabilizing activity of the peptide against all membranes, as assessed by a dye release assay, despite the fact that both peptides disturb either zwitterionic POPE or anionic POPG in mixed membranes to a similar degree. While the disruption of lipid acyl chains is likely to be important for the pore-forming activity of the peptide, it seems likely that other factors contribute. One such factor must be the α-helicity of the peptide, where the reduction of this secondary structure content in the truncated peptide inhibits its ability to form a pore. The antimicrobial and hemolytic peptide melittin, from bee venom, also has a strongly cationic C-terminal segment (Table 1) and has been studied in some detail (*34*). The structure of this peptide has been determined in phosphatidylcholine vesicles, and while the α-helical nature of the secondary structure is confirmed, the helix does not extend into the C-terminal segment, which remains essentially unstructured (*48*). The CD analysis in the present study indicates that both peptides adopt mostly α-helical conformations in 50% TFE, but the helical content is reduced in the presence of lipid vesicles, in particular for the truncated chrysophsin-ΔC. Therefore, contrary to what might have been expected, the RRRH sequence is also important for maintaining the helical nature of the peptide and its membrane-disrupting activity though it may itself not adopt a helical structure. However, it has been shown previously that positively charged residues stabilize C-terminal helix formation due to interactions with the negative end of the helix dipole (*49*). Balancing the apparently conflicting roles of the RRRH sequence may allow future peptides to be designed with modulated toxicity to eukaryotic cells.

Function of Chrysophsin in Nature. The data presented in the present study may also have important implications as to how antimicrobial peptides may be classified. In the original study describing the isolation and characterization of chrysophsin (*9*), a comparison between the primary sequences of the fish-derived peptides chrysophsin and misgurin (*50*) was made with that of melittin, a peptide found in bee venom (*51*). All three peptides have strongly cationic C-terminal segments, RRRK in the case of misgurin and KRKRQQ in the case of melittin. These similarities, and the toxicity of chrysophsin to eukaryotic fibroblasts and erythrocytes, suggest that chrysophsin might also have a role in defense against predation. The limited identity between chrysophsin and melittin in the remainder of the sequence prevents identification of the cationic C-terminal segment as the sole determinant of this activity, since a combination of other factors may also be important, but suggests further study of this motif is warranted.

ACKNOWLEDGMENT

A.J.M. thanks Peiman Shooshtarizaheh for mass spectrometris analysis of peptides and Thomas Ebbesen for access to the Flurolog 3-22. ISIS is acknowledged for hosting the laboratory.

REFERENCES

1. Brogden, K. A. (2005) Antimicrobial peptides: pore formers or metabolic inhibitors in bacteria? *Nat. Rev. Microbiol. 3*, 238−250.
2. Reddy, K. V. R., Yedery, R. D., and Aranha, C. (2004) Antimicrobial peptides: premises and promises, *Int. J. Antimicrob. Agents 24*, 536−547.
3. Marr, A. K., Gooderham, W. J., and Hancock, R. E. W. (2006) Antibacterial peptides for therapeutic use: obstacles and realistic outlook, *Curr. Opin. Pharmacol. 6*, 468−472.
4. Hancock, R. E. W., and Sahl, H-G. (2006) Antimicrobial and host-defence peptides as new anti-infective therapeutic strategies, *Nat. Biotechnol. 24*, 1551−1557.
5. Silphaduang, U., and Noga, E. J. (2001) Peptide antibiotics in mast cells of fish, *Nature 414*, 268−269.

6. Lauth, X., Shike, H., Burns, J. C., Westerman, M. E., Ostland, V. E., Carlberg, J. M., Van Olst, J. C., Nizet, V., Taylor, S. W., Shimizu, C., and Bulet, P. (2002) Discovery and characterization of two isoforms of moronecidin, a novel antimicrobial peptide from hybrid striped bass, *J. Biol. Chem. 277*, 5030−5039.
7. Shike, H., Lauth, X., Westerman, M. E., Ostland, V. E., Carlberg, J. M., Van Olst, J. C., Shimizu, C., Bulet, P., and Burns, J. C. (2002) Bass hepcidin is a novel antimicrobial peptide induced by bacterial challenge, *Eur. J. Biochem. 269*, 2232−2237.
8. Cole, A. M., Darouiche, R. O., Legarda, D., Connell, N., and Diamond, G. (2000) Characterization of a fish antimicrobial peptide: gene expression, subcellular localization, and spectrum of activity, *Antimicrob. Agents Chemother. 44*, 2039−2045.
9. Iijima, N., Tanimoto, N., Emoto, Y., Morita, Y., Uematsu, K., Murakami, T., and Nakai, T. (2003) Purification and characterization of three isoforms of chrysophsin, a novel antimicrobial peptide in the gills of the red sea bream *Chrysophrys major*, *Eur. J. Biochem. 270*, 675−686.
10. Zasloff, M. (1987) Magainins, a class of antimicrobial peptides from *Xenopus* skin: isolation, characterization of two active forms, and partial cDNA sequence of a precursor, *Proc. Natl Acad. Sci. U.S.A. 84*, 5449−5453.
11. Zhang, L., Parente, J., Harris, S. M., Woods, D. E., Hancock, R. E. W., and Falla, T. J. (2005) Antimicrobial peptide therapeutics for cystic fibrosis, *Antimicrob. Agents. Chemother. 49*, 2921−2927.
12. Mason, A. J., Chotimah, I. N. H., Bertani, P., and Bechinger, B. (2006) A spectroscopic study of the membrane interaction of the antimicrobial peptide Pleurocidin, *Mol. Membr. Biol. 23*, 185−194.
13. Saint, N., Cadiou, H., Bessin, Y., and Molle, G. (2002) Antibacterial peptide pleurocidin forms ion channels in planar lipid bilayers, *Biochim. Biophys. Acta 1564*, 359−364.
14. Patrzykat, A., Friedrich, C. L., Zhang, L., Mendoza, V., and Hancock, R. E. (2002) Sublethal concentrations of pleurocidin derived antimicrobial peptides inhibit macromolecular synthesis in *Escherichia coli*, *Antimicrob. Agents Chemother. 46*, 605−614.
15. Mason, A. J., Marquette, A., and Bechinger, B. (2007) Zwitterionic phospholipids and sterols modulate antimicrobial peptide induced membrane destabilisation, *Biophys. J.* doi:10.1529/biophysj.107.116681.
16. Leontiadou, H., Mark, A. E., and Marrink, S. J. (2006) Antimicrobial peptides in action, *J. Am. Chem. Soc. 128*, 12156−12161.
17. Hallock, K. J., Henzler Wildman, K., Lee, D.-K., and Ramamoorthy, A. (2002) An innovative procedure using a sublimable solid to align lipid bilayers for solid-state NMR studies, *Biophys. J. 82*, 2499−2503.
18. Sreerama, N., and Woody, R. W. (2000) Estimation of protein secondary structure from CD spectra: Comparison of CONTIN, SELCON and CDSSTR methods with an expanded reference set, *Anal. Biochem. 287*, 252−260.
19. Lindman, H. R. (1974) *Analysis of variance in complex experimental designs*, W. H. Freeman & Co., San Francisco, CA.
20. Davis, J. H. (1983) The description of membrane lipid conformation order and dynamics H-2-NMR, *Biochim. Biophys. Acta 737*, 117−171.
21. Schäfer, H., Mädler, B., and Volke, F. (1995) De-PAKE-ing of NMR powder spectra by nonnegative least-squares analysis with Tikhonov regularization, *J. Magn. Reson. 116*, 145−149.
22. Sternin, E., Bloom, M., and MacKay, A. L. (1983) De-PAKE-ing of NMR spectra, *J. Magn. Reson. 55*, 274−282.
23. Seelig, A., and Seelig, J. (1974) Dynamic structure of fatty acyl chains in a phospholipid bilayer measured by deuterium magnetic-resonance, *Biochemistry 13*, 4839−4845.
24. Alley, M. C., Scudiero, D. A., Monks, A., Hursey, M. L., Czerwinski, M. J., Fine, D. L., Abbott, B. J., Mayo, J. G., Shoemaker, R. H., and Boyd, M. R. (1988) Feasibility of drug screening with panels of human tumor cell lines using a microculture tetrazolium assay, *Cancer Res. 48*, 589−601.
25. Yang, N., Strøm, M. B., Mekonned, S. M., Svendsen, J. S., and Rekdal, Ø. (2004) The effects of shortening lactoferrin derived peptides against tumour cells, bacteria and normal human cells, *J. Pept. Sci. 10*, 37−46.
26. Mason, A. J., Gasnier, C., Kichler, A., Prévost, G., Aunis, D., Metz-Boutigue, M.-H., and Bechinger, B. (2006) Designed histidine-rich peptides show pH dependent antibiotic action against pathogenic bacteria peptides, *Antimicrob. Agents Chemother. 50*, 3305−3311.
27. Morein, S., Andersson, A-S., Rilfors, L., and Lindblom, G. (1996) Wild-type *Escherichia coli* cells regulate the membrane lipid composition in a "window" between gel and non-lamellar structures, *J. Biol. Chem. 271*, 6801−6809.
28. Mason, A. J., Bechinger, B., and Kichler, A. (2007) Rational design of vector and antibiotic peptides using solid-state NMR, *Mini Rev. Med. Chem. 7*, 491−497.
29. Bechinger, B., and Sizun, C. (2003) Alignment and structural analysis of membrane polypeptides by ^{15}N and ^{31}P solid-state NMR spectroscopy, *Concepts Magn. Reson. 18A*, 130−145.
30. Bechinger, B., Aisenbrey, C., and Bertani, P. (2004) The alignment, structure and dynamics of membrane-associated polypeptides by solid-state NMR spectroscopy, *Biochim. Biophys. Acta 1666*, 190−204.
31. Bechinger, B., Zasloff, M., and Opella, S. J. (1993) Structure and orientation of the antibiotic peptide magainin in membranes by solid-state nuclear magnetic resonance spectroscopy, *Protein Sci. 2*, 2077−2084.
32. Chekmenev, E. Y., Vollmar, B. S., Forseth, K. T., Manion, M. N., Jones, S. M., Wagner, T. J., Endicott, R. M., Kyriss, B. P., Homem, L. M., Pate, M., He, J., Raines, J., Gor'kov, P. L., Brey, W. W., Mitchell, D. J., Auman, A. J., Ellard-Ivey, M. J., Blazyk, J., and Cotton, M. (2006) Investigating molecular recognition and biological function at interfaces using piscidins, antimicrobial peptides from fish, *Biochim. Biophys. Acta 1758*, 1359−1372.
33. Bechinger, B. (1999) The structure, dynamics and orientation of antimicrobial peptides in membranes by multidimensional solid-state NMR spectroscopy, *Biochim. Biophys. Acta 1462*, 157−183.
34. Bechinger, B., and Lohner, K. (2006) Detergent-like actions of linear amphipathic cationic antimicrobial peptides, *Biochim. Biophys. Acta 1758*, 1529−1539.
35. Yoshida, K., Mukai, Y., Niidome, T., Takashi, C., Tokunaga, Y., Hatakeyama, T., and Aoyagi, H. (2001) Interaction of pleurocidin and its analogs with phospholipids membrane and their antibacterial activity, *J. Pept. Res. 57*, 119−126.
36. Yandek, L. E., Pokorny, A., Florén, A., Knoelke, K., Langel, Ü., and Almeida, P. F. F. (2007) Mechanism of the cell-penetrating peptide Tp10 permeation of lipid bilayers, *Biophys. J. 92*, 2434−2444.
37. Mason, A. J., Martinez, A., Glaubitz, C., Danos, O., Kichler, A., and Bechinger, B. (2006) The antibiotic and DNA transfecting peptide LAH4 selectively associates with, and disorders, anionic lipids in mixed membranes, *FASEB J. 20*, 320−322; doi:10.1096/fj.05-4293fje.
38. Bechinger, B. (2005) Detergent-like properties of magainin antibiotic peptides: A ^{31}P solid-state NMR spectroscopy study, *Biochim. Biophys. Acta 1712*, 101−108.
39. Bechinger, B., Kinder, R., Helmle, M., Vogt, T. C., Harzer, U., and Schinzel, S. (1999) Peptide structural analysis by solid-state NMR spectroscopy, *Biopolymers 51*, 174−190.
40. Eliassen, L. T., Berge, G., Leknessund, A., Wikman, M., Lindin, I., Løkke, C., Ponthan, F., Johnsen, J. I., Sveinbjørssen, B., Kogner, P., Flægstad, T., and Rekdal, Ø. (2006) The antimicrobial peptide, Lactoferricin B, is cytotoxic to neuroblastoma cells *in vitro*, and inhibits xenograft growth *in vivo*, *Int. J. Cancer 119*, 493−500.
41. Utsugi, T., Schroit, A. J., Connor, J., Bucana, C. D., and Fidler, I. J. (1991) Elevated expression of phosphatidylserine in the outer membrane leaflet of human tumor cells and recognition by activated human blood monocytes, *Cancer Res. 51*, 3062−3066.
42. Mason, A. J., Moussaoui, W., Abdelrahman, T., Bertani, P., Marquette, A., Shooshtarizaheh, P., Moulay, G., Boukhari, A., Guerold, B., Kichler, A., Metz-Boutigue, M.-H., Candolfi, E., Prévost, G., and Bechinger, B. Structural determinants of antimicrobial and antiplasmodial activity and selectivity in histidine rich amphipathic cationic peptides (manuscript in preparation).
43. Huschtscha, L. I., and Holliday, R. (1983) Limited and unlimited growth of SV40-transformed cells from human diploid MRC-5 fibroblasts, *J. Cell. Sci. 63*, 77−99.
44. Daum, G., and Vance, J. E. (1997) Import of lipids into mitochondria, *Prog. Lipid Res. 36*, 103−130.
45. Mitchell, D. J., Kim, D. T., Steinman, L., Fathman, C. G., and Rothbard, J. B. (2000) Polyarginine enters cells more efficiently than other polycationic homopolymers, *J. Pept. Res. 56*, 318−325.
46. Bechinger, B. (2004) Structure and function of membrane-lytic peptides, *Crit. Rev. Plant Sci. 23*, 271−292.

47. McLaughlin, S. (1989) The electrostatic properties of membranes, *Annu. Rev. Biophys. Biophys. Chem. 18*, 113−136.
48. Okada, A., Wakamatsu, K., Miyazawa, T., and Higashijimal, T. (1994) Vesicle-bound conformation of melittin: transferred nuclear Overhauser enhancement analysis in the presence of perdeuterated phosphatidylcholine vesicles, *Biochemistry 33*, 9438−9446.
49. Bechinger, B., Zasloff, M., and Opella, S. J. (1998) Structure and dynamics of the antibiotic peptide PGLa in membranes by solution and solid-state nuclear magnetic resonance spectroscopy, *Biophys. J. 74*, 981−987.
50. Park, C. B., Lee, J. H., Park, I. Y., Kim, M. S., and Kim, S. C. (1997) A novel antimicrobial peptide from the loach, *Misgurnus anguillicaudatus*, *FEBS Lett. 411*, 173−178.
51. Dempsey, C. E. (1990) The actions of melittin on membranes, *Biochim. Biophys. Acta 1031*, 143−161.

BI701344M